PCCP

RSC Publishing

PAPER

View Article Online
View Journal | View Issue



Cite this: *Phys. Chem. Chem. Phys.*, 2013, **15**, 17468

# Electron correlation and relativistic effects in the secondary NMR isotope shifts of $CSe_2$†

Perttu Lantto,*[a] Sanna Kangasvieri[b] and Juha Vaara[a]

Received 6th May 2013,
Accepted 12th August 2013

DOI: 10.1039/c3cp51904j

**www.rsc.org/pccp**

Secondary isotope effects on nuclear shielding provide an experimentally well-defined reference point of quantum-chemical methodology. We carry out a quantum-mechanical treatment of thermal rovibrational motion in the linear $CSe_2$ molecule and combine it with relativistic modeling of $^{77}Se$ and $^{13}C$ nuclear magnetic shieldings. The effects of electron correlation are studied at nonrelativistic (NR) *ab initio* and both NR and relativistic density functional theory (DFT) levels. Fully relativistic 4-component Dirac-DFT (D-DFT) as well as Breit–Pauli perturbation theory (BPPT) are used to produce the relativistic shielding surfaces. Quantitative agreement with the experimental secondary isotope effects can be obtained by a piecewise combination of a high-level *ab initio* NR shielding surface with the more approximate, albeit reasonable-quality relativistic corrections by DFT at either Dirac or BPPT levels of theory, when operating at the basis-set limit. Using a high-quality potential energy surface is also crucial, which further underlines the highly demanding nature of modeling of the isotope shifts.

## 1 Introduction

Low-density gas-phase experiments for molecular properties are usually not available. They would be the preferred choice for comparing with the results of molecular electronic structure theory. In such comparisons one needs to take into account the rovibrational motion of the molecule. Secondary isotope shifts of nuclear magnetic resonance (NMR) shielding constants are due to the mass change of another nucleus in the molecule.[1] They are entirely quantum-mechanical (meaning classically non-existing) parameters arising from the fact that the different isotopomers have different rovibrational states and, hence, rovibrationally averaged properties. In $CSe_2$, the secondary isotope shifts of the heavy $^{77}Se$ nucleus arise due to the isotope change of either the C atom, *e.g.*,

$$^{1}\Delta^{77}\mathrm{Se}(^{13/12}\mathrm{C}) = \sigma_{\mathrm{Se}}(^{77}\mathrm{Se}{=}{=}^{13}\mathrm{C}{=}{=}^{80}\mathrm{Se}) - \sigma_{\mathrm{Se}}(^{77}\mathrm{Se}{=}{=}^{12}\mathrm{C}{=}{=}^{80}\mathrm{Se}), \quad (1)$$

or the other Se atom (with $M$ denoting a certain Se isotope),

$$^{2}\Delta^{77}\mathrm{Se}(^{M/76}\mathrm{Se}) = \sigma_{\mathrm{Se}}(^{77}\mathrm{Se}{=}{=}^{12}\mathrm{C}{=}{=}^{M}\mathrm{Se}) - \sigma_{\mathrm{Se}}(^{77}\mathrm{Se}{=}{=}^{12}\mathrm{C}{=}{=}^{76}\mathrm{Se}). \quad (2)$$

Secondary isotope shifts are dominated by intramolecular phenomena, thus being insensitive to solvent effects. In the field of NMR theory they constitute, therefore, a more suitable point of comparison for the theoretical modeling of rovibrational effects than, *e.g.*, the thermal effects on the absolute shielding constants or chemical shifts. In a solvated molecule the latter properties are much more sensitive to intermolecular interactions, which are challenging to model quantitatively.[2–5]

Accounting for zero-point vibrational (ZPV) corrections is increasingly routine in the modeling of NMR spectroscopic parameters.[6–8] Although there exist semi-automated methods for treating ZPV in connection with nonrelativistic (NR) computations, only a few studies have been published on nuclear motion effects on relativistic (REL) heavy-element NMR shieldings.[5,9–13] Furthermore, a treatment of finite-temperature effects is far less common: especially comprehensive quantum-mechanical treatments of heavy-element compounds are few and far between.[5] So far, the finite-temperature effects on magnetic properties, such as magnetizabilities and rotational $\boldsymbol{g}$-tensors[14] as well as on the NMR shieldings and their isotope shifts,[3–5,15–17] have usually been demonstrated for light elements. The main relativistic corrections to light-atom NMR shieldings due to spin–orbit (SO) interactions[18–21] have long been known to be sensitive to rovibrational motion.[4,22,23] A full treatment of

[a] *NMR Research Group, Department of Physics, P.O. Box 3000, FI-90014 University of Oulu, Finland. E-mail: perttu.lantto@oulu.fi*
[b] *Laboratory of Physical Chemistry, Department of Chemistry, P.O. Box 55 (A.I. Virtasen aukio 1), FIN-00014 University of Helsinki, Finland*

† Electronic supplementary information (ESI) available: Relativistic BPPT contributions to nuclear shielding constants and anisotropies, temperature derivatives of the secondary isotope shifts and shielding constants in $CSe_2$ at room temperature, nuclear shielding hypersurfaces at both BPPT and 4-component Dirac levels of theory. Also more detailed illustrations of the temperature dependence of the secondary isotope shifts and shielding constants, the main relativistic BPPT-5 effects on them, as well as their individual rovibrational contributions. See DOI: 10.1039/c3cp51904j

finite-temperature rovibrational effects on shieldings and the secondary isotope effects in the case of the light $^{13}$C nucleus was shown to be necessary in $CX_2$ (X = O–Te) systems.[3,4] When also scalar relativistic (SR) effects were included, an approach at this level of detail provided a quantitative description of the experimental normal halogen dependence of $^{13}$C and $^{1}$H shieldings in $CH_3X$ (X = F–I).[17]

The NMR parameters generally pose serious demands for the description of electron correlation. Also, for heavier than 1st-row elements not only valence but also semi-core correlation is needed for hyperfine parameters.[24] The mostly reasonable performance of the computationally appealing density-functional theory (DFT) has been noted to often arise from a favorable error cancellation in the calculations of NMR tensors.[25,26] There exist, however, DFT functionals that fare rather well for also the absolute values of hyperfine properties, for instance KT2[27] in the case of NMR shieldings in systems containing light elements.[28] Concerning heavy-atom systems there is mounting evidence obtained by benchmarking DFT results against coupled-cluster singles and doubles with perturbative triples [CCSD(T)] data that the NR shielding is, in fact, more sensitive to the electron correlation treatment than the REL contribution.[5,29–32] DFT shielding calculations of heavy nuclei appear to be susceptible to (at times) appreciable errors originating already at the NR level. In particularly difficult electron correlation cases also the relativistic corrections themselves should be computed at a correlated *ab initio* level.[29,31]

As there exist so far no practical, fully relativistic and correlated *ab initio* methods for second-order magnetic properties (such as nuclear shielding), the only available *ab initio* method for benchmarking DFT at the REL level is provided by Breit–Pauli perturbation theory (BPPT)[33–35] or the corresponding linear response-elimination of the small component (LR-ESC) method.[36,37] These methods treat relativistic interactions as corrections on top of the NR state. There is accumulating and compelling evidence from several BPPT studies[5,29–35,38–44] of both light- and heavy-element NMR shieldings in many kinds of (even fairly exotic) molecules containing up to 6th row elements, that the major part of the relativistic effect on chemical shift (as well as shielding anisotropy) is mainly due to five perturbational contributions, collectively denoted as BPPT-5.[5,29–32,40,43] The five terms can be grouped into SR paramagnetic (REL-*p*) and spin–orbit (SO-I) terms.[45,46] The other BPPT terms are practically ''atomic'', isotropic core-like contributions,[29,30] insensitive to both electron correlation and chemical environment. Therefore, they do not contribute significantly to the relative chemical shift or anisotropic parameters. The BPPT-5 terms have also been shown to be responsible for the relativistic rovibrational corrections of both the light-[17] and heavy-element[5] shieldings. For heavy-element shifts, not only the SO-I terms, but also the SR REL-*p* effects contribute significantly to the rovibrational averages.[5]

In this paper we extend the relativistic quantum-mechanical modeling of rovibrational effects of heavy-element compounds to $^{77}$Se shielding in $CSe_2$, for which experimental secondary isotope shifts were obtained in ref. 3. There, reasonably good correspondence was obtained between fairly modest NR-level modeling of nuclear shielding and experimental secondary isotope shifts of $^{77}$Se. This is counterintuitive, as the corresponding properties of the light $^{13}$C nucleus were later shown to necessitate a relativistic treatment.[4] The reason for this apparent inconsistency is investigated presently. The $CSe_2$ molecule with its double bonds is expected to feature respectable electron correlation effects. Hence, we subject them to a thorough scrutiny. At the same time we obtain a more detailed picture of both correlation and relativistic effects on the rovibrational parameters of also $^{13}$C, as compared to the earlier study reported in ref. 4. As in ref. 5, a high-level *ab initio* cubic anharmonic force field is produced to calculate accurate thermal averages of the displacement coordinates that characterise nuclear motion at finite temperature. In the method used presently, these averages are combined in a Taylor series expansion of the shielding hypersurface around the equilibrium geometry, with parameters obtained either at fully relativistic, perturbational BPPT, or NR levels.

## 2 Computational details

To obtain the harmonic and leading anharmonic vibrational corrections, one needs the harmonic and cubic anharmonic molecular force fields. For the linear Se=C=Se molecule, a convenient basis for expressing the force field is provided by the two bond lengths, $r$ and $r'$, as well as the bond angle within two perpendicular planes, $\theta$ and $\theta'$. The full third-order potential energy surface in these curvilinear internal coordinates

$$\begin{aligned} V &= \frac{1}{2} f_{rr}\left[(\Delta r)^2 + (\Delta r')^2\right] + f_{rr'}\Delta r\Delta r' \\ &+ \frac{1}{2} f_{\theta\theta}\left[(\Delta\theta)^2 + (\Delta\theta')^2\right] \\ &+ \frac{1}{6} f_{rrr}\left[(\Delta r)^3 + (\Delta r')^3\right] \\ &+ \frac{1}{2} f_{rrr'}\Delta r\Delta r'(\Delta r + \Delta r') \\ &+ \frac{1}{2} f_{r\theta\theta}(\Delta r + \Delta r')\left[(\Delta\theta)^2 + (\Delta\theta')^2\right], \end{aligned} \tag{3}$$

was fitted to total energies computed at 45 displaced geometries in the close vicinity of the equilibrium geometry.[3,4,14,15,17] The energy points were calculated at the CCSD(T) level using an energy-consistent scalar-relativistic pseudopotential (ECP10MDF)[47] for the Se atoms, with the corresponding cc-pVQZ and cc-pV5Z valence basis sets. The light C atom was equipped with the corresponding all-electron basis sets, cc-pVQZ and cc-pV5Z.[48] These combinations are here denoted as VQZ and V5Z, respectively.

The NR shielding tensors at equilibrium geometry, $r_e$, as well as the shielding constant hypersurfaces

$$\begin{aligned}\langle\sigma\rangle^T &= \sigma_e + \sigma_r\langle\Delta r\rangle^T + \sigma_{r'}\langle\Delta r'\rangle^T \\ &\quad + \frac{1}{2}\sigma_{rr}\left\langle(\Delta r)^2\right\rangle + \frac{1}{2}\sigma_{r'r'}\left\langle(\Delta r')^2\right\rangle^T \\ &\quad + \sigma_{rr'}\langle\Delta r\Delta r'\rangle^T + \sigma_{\theta\theta}\left\langle(\Delta\theta)^2\right\rangle^T \\ &= \sigma_e + \langle\sigma_r\rangle^T + \langle\sigma_{r'}\rangle^T + etc.\end{aligned} \quad (4)$$

up to second-order terms in the displacement coordinates were computed at Hartree–Fock (HF) and second-order Møller–Plesset perturbation theory (MP2), as well as CCSD and CCSD(T) levels of theory with the parallel CFOUR code.[49] In eqn (4), the expansion of shielding has been thermally averaged at temperature $T$, causing the appearance of the average displacement coordinates $\langle R_i\rangle^T$ and $\langle R_iR_j\rangle^T$. Their computation is explained in more detail in ref. 3, 4 and 17. The angle degeneracy due to the equivalent $\theta$ and $\theta'$ coordinates has been included in the last term. In addition, the Dirac code[50] was used for four-component relativistic calculations using the simple magnetic balance ansatz.[51] DFT with the B3LYP[52,53] exchange–correlation functional (denoted as D-B3LYP) was used. In both the NR and 4-component relativistic shielding calculations, the gauge-including atomic orbital (GIAO) ansatz was employed. The Dalton quantum chemistry program[54] was used to calculate all the 16 relativistic BPPT terms[33–35] in the $^{77}$Se and $^{13}$C shielding tensors. DFT computations of the BPPT contributions to the shielding hypersurface were carried out with the KT2[27] functional, as well as the generic BLYP,[53,55] B3LYP, and BHandHLYP[53,56] series of functionals. The first two feature 0% of exact HF exchange admixture while the latter two have 20%, and 50%, respectively.

In the all-electron NR shielding calculation, the Huzinaga–Kutzelnigg HIV basis set[57,58] was used for C. The structure of this basis set is [11s7p3d1f/8s7p3d1f] in the [primitive/contracted] notation. A corresponding FIV basis set, [16s13p12d2f/13s12p12d2f], was constructed for the Se atom in the spirit of Huzinaga–Kutzelnigg basis sets from Fægri's exponents for a one-component basis set,[59] supplemented with polarization functions and contracted analogously to HIV. Uncontracted HIVu6/FIVu6 basis sets (17s13p3d1f)/(22s19p18d2f) were used for C/Se atoms in the relativistic BPPT and D-B3LYP (the indicated basis sets used for the large component) shielding calculations. These sets were obtained by adding six sets of tight sp/spd functions to the uncontracted HIV/FIV sets of C/Se. This procedure is shown to provide almost fully converged light atom and Xe NMR shielding tensors, as well as individual BPPT contributions thereto, in Xe molecules.[5,29,31]

### 2.1 Equilibrium geometry and the force field

The cubic anharmonic force field for $CSe_2$ is given in Table 1. For this molecule, the CCSD(T)/V5Z-level of theory provides the best theoretical results so far, as seen in the comparison with experiment. Especially, the harmonic asymmetric stretching and bending frequencies are improved as compared to the VQZ basis set level, although the latter produces accidentally better $r_e$ bond lengths.

**Table 1** Equilibrium geometry, harmonic frequencies as well as harmonic and cubic anharmonic force constants for $CSe_2$[a]

| | MP2[b] | DFT[c] | CCSD(T)[d] | CCSD(T)[e] | Exp.[f] |
|---|---|---|---|---|---|
| $r_e$ | 1.7053 | 1.689 | 1.6890 | 1.6881 | 1.6919 |
| $\omega_1$ | 371.84 | 381.78 | 314.08 | 379.97 | 374.48 |
| $\omega_2$ | 299.65 | 307.06 | 380.55 | 309.40 | 302.89 |
| $\omega_3$ | 1295.54 | 1305.01 | 1287.68 | 1292.68 | 1254.30 |
| $f_{rr}$ | 6.228 | 6.448 | 6.346 | 6.359 | 6.088 |
| $f_{rr'}$ | 0.282 | 0.415 | 0.472 | 0.439 | 0.515 |
| $f_{\theta\theta}$ | 0.463 | 0.476 | 0.498 | 0.483 | 0.465 |
| $f_{rrr}$ | −29.737 | −36.053 | −39.755 | −34.167 | |
| $f_{rrr'}$ | −0.810 | −0.878 | −1.064 | −0.665 | |
| $f_{r\theta\theta}$ | −0.477 | −0.581 | −0.727 | −0.581 | |

[a] Frequencies (in $cm^{-1}$ units) for the $^{13}C^{80}Se_2$ isotopomer. Geometry and force constants in units of aJ, Å, and rad. [b] Ref. 4. [c] DFT result with LDA functional from ref. 3. [d] Present work. Force field computed with the cc-pVQZ valence basis set and the corresponding scalar relativistic ECP for Se. [e] Present work. Force field computed with the cc-pV5Z valence basis set and the corresponding scalar relativistic ECP for Se. [f] Ref. 60.

## 3 Results and discussion

### 3.1 Correlation and relativistic effects at equilibrium geometry: DFT performance

Table 2 details the calculated results for the shielding tensors at the equilibrium geometry. There are notable correlation effects on non-relativistic $^{13}$C shielding constant and anisotropy in $CSe_2$. As compared to the best current level, CCSD(T), the performance of MP2 is quite modest and at least CCSD is needed for a reasonable correlation treatment. DFT estimates moderately the $^{13}$C shielding parameters, the best functional being the pure generalized gradient approximation (GGA) KT2. For the $^{77}$Se shielding parameters, however, DFT gives correlation effects mostly with the wrong sign. We compare the NR DFT shielding surfaces to both CCSD and CCSD(T) results below.

We turn to relativistic effects as seen in Table 2, for which DFT provides reasonable estimates as judged by the fact that the results with different GGA and hybrid functionals fall in a narrow range. Hence, they all should suffice for treating the relativistic corrections. We choose to discuss the relativistic effects with the most familiar B3LYP functional in what follows. The 4-component D-B3LYP relativistic level of theory is considered to provide the best current estimations. Relativistic effects play only a moderate role in the $^{77}$Se shielding parameters as they amount to *ca.* 13% and 4% of the corresponding $\sigma_{Se}^{NR}$ and $\Delta\sigma_{Se}^{NR}$, respectively. However, the relativistic corrections are decisive for the $^{13}$C shielding tensor with *ca.* −71% and −9% contributions, respectively. The comparison of BPPT(B3LYP) with 4-component D-B3LYP results confirms that the former provides reliable relativistic corrections.

The differences in the BPPT-5 (BPPT-6 for $\Delta\sigma$) approximation from the total relativistic effect at the BPPT level (including all the terms, see Tables S1 and S2 in ESI†) reveal that it is justified

 

**Table 2** Electron correlation dependence of calculated, nonrelativistic (NR) and relativistic (REL) shielding constants $\sigma$ and anisotropies $\Delta\sigma$ in $CSe_2$ at equilibrium geometry[a]

| Method | $\sigma_C$ | $\Delta\sigma_C$ | $\sigma_{Se}$ | $\Delta\sigma_{Se}$ |
|---|---|---|---|---|
| Nonrelativistic (NR)[b] | | | | |
| HF | −130.6 | 638.3 | 1556.1 | 2178.9 |
| MP2 | −7.7 | 459.0 | 1787.4 | 1830.5 |
| CCSD | −68.2 | 548.1 | 1658.8 | 2023.9 |
| CCSD(T) | −44.4 | 513.1 | 1690.1 | 1976.9 |
| DFT/KT2 | −36.7 | 506.3 | 1575.9 | 2159.2 |
| DFT/BLYP | −63.8 | 542.8 | 1486.1 | 2283.1 |
| DFT/B3LYP | −79.4 | 565.2 | 1491.0 | 2275.9 |
| DFT/BHandHLYP | −101.6 | 597.2 | 1504.2 | 2256.7 |
| Relativistic contributions (REL)[c] | | | | |
| BPPT(1)/KT2 | 35.8 | −49.5 | 206.5 | 70.9 |
| BPPT(1)/BLYP | 36.7 | −50.5 | 202.1 | 76.1 |
| BPPT(1)/B3LYP | 37.4 | −52.0 | 203.7 | 74.2 |
| BPPT(1)/BHandHLYP | 39.3 | −55.1 | 207.0 | 70.0 |
| BPPT(1 + 2)/B3LYP | 33.2 | −45.3 | 196.4 | 83.3 |
| D-B3LYP[d] | 33.0 | −50.1 | 219.2 | 78.4 |
| BPPT-5(1)/B3LYP[e] | 36.2 | −51.6 | −64.4 | 75.5 |
| BPPT-5(1 + 2)/B3LYP[e] | 32.0 | −44.9 | −71.7 | 84.6 |
| Total (NR + REL) | | | | |
| CCSD(T) + D-B3LYP | −11.3 | 463.0 | 1909.3 | 2055.2 |
| BPPT/KT2 | −0.9 | 456.8 | 1782.4 | 2230.1 |
| BPPT/BHandHLYP | −62.3 | 542.2 | 1711.2 | 2326.8 |
| Basis set correction[f] | −2.4 | 3.7 | −1.0 | 1.6 |
| Rovib. corr.[g] | −1.5 | | −34.9 | |
| | (−2.6) | | (−32.8) | |
| Theor.[h] | −15.3 | 466.6 | 1873.4 | 2056.8 |
| Experimental[i] | | | | |
| Gas[62] | | | 1826.0 | |
| Liquid[3] | −17.8 | | | |
| Liquid[63] | | | 1769.2 | |
| Liquid crystal[64] | −16.9(5) | 506(30) | | 2210(120) |
| Solid[65] | −21.8 | 506.0 | | |

[a] In ppm. For $r_e$(C–Se) = 1.6881 Å obtained at the CCSD(T)/cc-pV5Z level. The BPPT anisotropies with respect to the symmetry axis, $\Delta\sigma = \sigma_{||} - \sigma_{\perp}$, contain also the SOS contribution, $\Delta\sigma^{SOS} = -3\sigma_{||}^{SD\text{-}I(1)}$, of ref. 46 as appropriate for a linear molecule. [b] With the HIV/FIV basis set for C/Se. [c] All relativistic calculations at the DFT level with the HIVu6/FIVu6 basis set for C/Se. In the BPPT calculations, the common gauge origin was placed at the nucleus in question. (1) denotes that only the one-electron spin–orbit contributions are included. (1 + 2) denotes that both 1- and 2-electron contributions are used. In the case of 4-component calculations, the relativistic contributions are obtained as D-DFT – NR-DFT. [d] Relativistic 4-component D-DFT calculation. [e] BPPT-5 (BPPT-6 for $\Delta\sigma$) approximation with the numerically most important five (six) relativistic terms affecting chemical shift and anisotropic parameters, see ref. 45. The isotropic core terms, important for absolute shielding, are neglected. [f] Change in the NR part from the HIV/FIV to HIVu6/FIVu6 basis set at the DFT(B3LYP) level. [g] Rovibrational correction at the NR[CCSD(T)] + REL[D-B3LYP] level for the $^{77}Se{=}^{13}C{=}^{80}Se$ isotopomer at $T$ = 300 K. NR part in parenthesis. [h] NR[CCSD(T)] + REL[D-B3LYP] (+ rovibrational correction at $T$ = 300 K for shielding constants). [i] Converted to the absolute shielding (see ref. 3) by using $\sigma_C$(300 K) = 195.1 ppm and $\sigma_{Se}$=2069 ppm for the internal $CH_4$ and $(CH_3)_2Se$ (liquid) reference molecules for $^{13}C$ and $^{77}Se$, respectively, from ref. 61.

to use the major terms only, and neglect the rest. The two-electron SO-I terms in the BPPT(1 + 2)/B3LYP result make reasonably large, several percent, contribution to the relativistic effect on $\sigma_{Se}$ and $\Delta\sigma_{Se}$. For the light C atom, the third-order SO (SO-I) terms, particularly the Fermi contact term therein, are dominating, while the SR terms (REL-$p$) play a smaller but non-negligible role. For the heavy Se nucleus these roles are interchanged as the SO-I terms experience strong mutual cancellation and, thus, leave the command for the REL-$p$ contributions. Therefore, despite the sizable relativistic contribution to $\sigma_{Se}$, the smallness of the resultant of the BPPT-5 terms (due to SO-I) already implies that, in this molecule, relativity may have a quite small role also in the rovibrational contributions to $\sigma_{Se}$ and its isotope shifts. It will be shown below that this, indeed, is the case.

### 3.2 Secondary $^{77}$Se isotope shifts

In $CSe_2$, the secondary isotope shifts have been measured for several isotopomers in ref. 3. The computed secondary isotope shifts for the same isotopomers are compared with the experimental data at $T$ = 300 K, in Table 3. Fig. 1 shows the temperature dependence of the spectral splitting between the E and D lines of the $^{77}$Se NMR spectrum [E–D splitting: $^2\Delta^{77}Se(^{80/78}Se) = \sigma_{Se}(^{77}Se{=}^{12}C{=}^{80}Se) - \sigma_{Se}(^{77}Se{=}^{12}C{=}^{78}Se)$] at different levels of theory, as well as the experimental results around room temperature.[3] The same information for the $^{77}$Se secondary isotope shift due to the change in the carbon isotope [E′–E splitting: $^1\Delta^{77}Se(^{13/12}C) = \sigma_{Se}(^{77}Se{=}^{13}C{=}^{80}Se) - \sigma_{Se}(^{77}Se{=}^{12}C{=}^{80}Se)$] is displayed in Fig. 2.

As expected, already the NR contribution to the isotope shifts is heavily dependent on the electron correlation treatment. The MP2 method underestimates them very clearly, and CCSD overestimates by more than 10%, when compared to the benchmark CCSD(T) data. The currently tested DFT functionals give a large range of results starting from a small overestimation by the pure DFT(GGA) functionals to a drastic exaggeration by the hybrid BHandHLYP functional. The KT2 GGA functional, designed for light-element NMR shieldings, performs best amongst the tested DFT functionals.

Relativistic effects increase the $^{77}$Se secondary isotope shifts by *ca.* 5–7%. Although small, they are needed to bring the computed shifts into a quantitative agreement with the experimental results.[3] The best DFT functional, KT2 as judged by the NR results, agrees with the BLYP result for the REL effect of E–D splitting (Fig. 1b) but in the E′–E case (Fig. 2b), KT2 produces a similar REL correction as the B3LYP functional. There are similar relative differences between the DFT functionals in the REL correction to that at the NR level of theory. However, the errors in the total secondary isotope shifts of $^{77}$Se behave systematically as a function of the exact HF exchange and, more importantly, the REL corrections are overall rather small. This indicates that the DFT results provide reasonable estimations of the REL correction with any current DFT functional.

B3LYP was used in fully relativistic, 4-component Dirac-DFT calculations (D-B3LYP) from which REL corrections (D-B3LYP-NR-B3LYP) were obtained. The corresponding BPPT(B3LYP) results with only the 1-electron SO-I terms underestimate the relativistic corrections to isotope shifts by about 20%. As noticed earlier in ref. 5, the sc. BPPT-5 terms are almost fully responsible for these 1-electron relativistic contributions. Including the 2-electron spin-same- (SSO) and spin-other-orbit (SOO) contributions at the BPPT(1 + 2) level clearly narrows the gap to the D-B3LYP results. However, as D-B3LYP does not

**Table 3** Experimental and theoretical secondary $^{77}$Se isotope shifts in $CSe_2$ at 300 K[a]

| NR[b] | Line[c] | KT2 | BLYP | B3LYP | BHandHLYP | MP2 | CCSD | CCSD(T) | CCSD(T)/VQZ[d] |
|---|---|---|---|---|---|---|---|---|---|
| $^1\Delta^{77}Se(^{13/12}C)$[e] | E′ | 607.0 | 640.9 | 685.1 | 744.6 | 453.6 | 628.9 | 564.9 | 616.8 |
| $^2\Delta^{77}Se(^{74/76}Se)$[f] | A | −17.1 | −17.8 | −19.6 | −22.2 | −9.6 | −19.4 | −16.5 | −18.6 |
| $^2\Delta^{77}Se(^{77/76}Se)$[f] | C | 8.3 | 8.6 | 9.4 | 10.7 | 4.6 | 9.4 | 8.0 | 9.0 |
| $^2\Delta^{77}Se(^{78/76}Se)$[f] | D | 16.3 | 16.9 | 18.6 | 21.2 | 9.1 | 18.5 | 15.7 | 17.7 |
| $^2\Delta^{77}Se(^{80/76}Se)$[f] | E | 31.8 | 33.1 | 36.3 | 41.3 | 17.7 | 36.0 | 30.7 | 34.6 |
| $^2\Delta^{77}Se(^{82/76}Se)$[f] | F | 46.5 | 48.4 | 53.2 | 60.5 | 26.0 | 52.8 | 44.9 | 50.6 |
| REL[g] | | KT2 | BLYP | B3LYP | BHandHLYP | B3LYP-5[h] | B3LYP(1&2)[i] | D-B3LYP[j] | D-B3LYP/VQZ[d,j] |
| $^1\Delta^{77}Se(^{13/12}C)$[e] | E′ | 20.7 | 21.9 | 20.6 | 17.4 | 20.9 | 25.5 | 26.9 | 28.0 |
| $^2\Delta^{77}Se(^{74/76}Se)$[f] | A | −0.7 | −0.7 | −0.8 | −0.9 | −0.8 | −0.9 | −1.0 | −1.1 |
| $^2\Delta^{77}Se(^{77/76}Se)$[f] | C | 0.3 | 0.3 | 0.4 | 0.4 | 0.4 | 0.4 | 0.5 | 0.5 |
| $^2\Delta^{77}Se(^{78/76}Se)$[f] | D | 0.6 | 0.6 | 0.7 | 0.9 | 0.7 | 0.8 | 0.9 | 1.0 |
| $^2\Delta^{77}Se(^{80/76}Se)$[f] | E | 1.2 | 1.2 | 1.4 | 1.7 | 1.4 | 1.6 | 1.8 | 2.0 |
| $^2\Delta^{77}Se(^{82/76}Se)$[f] | F | 1.8 | 1.8 | 2.1 | 2.5 | 2.1 | 2.4 | 2.7 | 3.0 |
| TOTAL[k] | | KT2 | BLYP | B3LYP | BHandHLYP | D-B3LYP | CCSD(T) + D-B3LYP | CCSD(T) + D-B3LYP/VQZ[d] | Exp.[c] |
| $^1\Delta^{77}Se(^{13/12}C)$[e] | E′ | 627.7 | 662.7 | 705.7 | 762.1 | 712.3 | 591.8 | 644.8 | 628.1 |
| $^2\Delta^{77}Se(^{74/76}Se)$[f] | A | −17.8 | −18.5 | −20.3 | −23.2 | −20.5 | −17.5 | −19.7 | −18.4 |
| $^2\Delta^{77}Se(^{77/76}Se)$[f] | C | 8.6 | 8.9 | 9.8 | 11.2 | 9.9 | 8.4 | 9.5 | 9.0 |
| $^2\Delta^{77}Se(^{78/76}Se)$[f] | D | 16.9 | 17.6 | 19.3 | 22.0 | 19.6 | 16.7 | 18.8 | 17.6 |
| $^2\Delta^{77}Se(^{80/76}Se)$[f] | E | 33.0 | 34.3 | 37.7 | 43.0 | 38.2 | 32.5 | 36.6 | 34.4 |
| $^2\Delta^{77}Se(^{82/76}Se)$[f] | F | 48.3 | 50.2 | 55.3 | 63.0 | 55.9 | 47.6 | 53.6 | 50.5 |

[a] In ppb. Present data with the CCSD(T)/V5Z force field with $r_e$ = 1.6881 Å unless otherwise noted. [b] Present nonrelativistic (NR) calculations with the HIV/FIV basis set for C/Se. [c] Experimental spectral lines as denoted in ref. 3, measured in $C_6D_6$ solution. [d] Present calculations with the CCSD(T)/VQZ force field with $r_e$ = 1.6890 Å. [e] See eqn (1). [f] See eqn (2). [g] Present relativistic (REL) contribution computed with the HIVu6/FIVu6 basis set for C/Se. Computed at the 1-electron BPPT level of theory unless otherwise noted. [h] Present results including only the main 1-electron relativistic BPPT-5 terms.[45] [i] Present relativistic BPPT contribution including both 1- and 2-electron SO-I terms. [j] Present four-component D-DFT relativistic contributions with the B3LYP functional (D-B3LYP − NR-B3LYP). [k] Present total isotope shift (TOTAL = NR + REL).

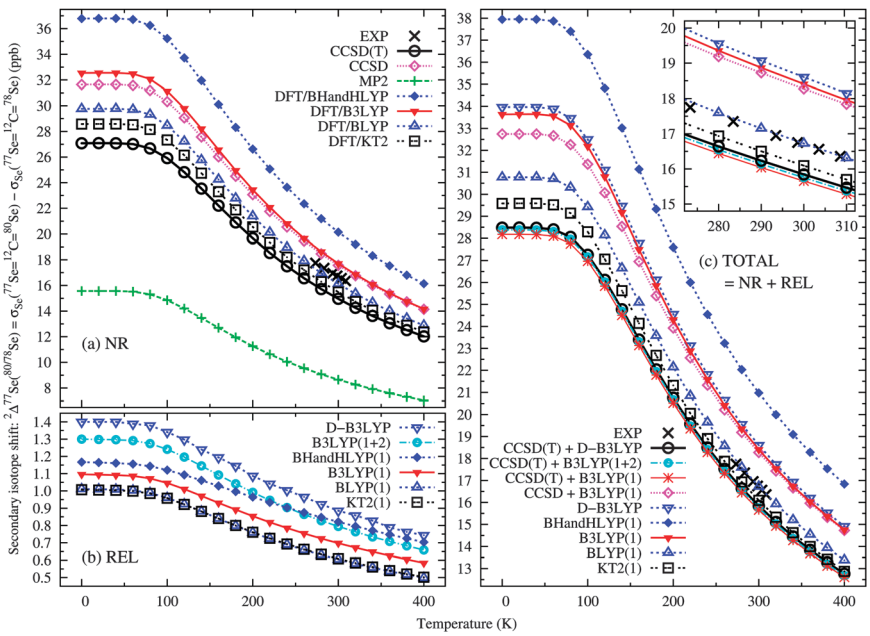


**Fig. 1** The two-bond secondary $^{77}$Se isotope shift: $^2\Delta^{77}Se(^{80/78}Se) = \sigma_{Se}(^{77}Se{=}^{12}C{=}^{80}Se) - \sigma_{Se}(^{77}Se{=}^{12}C{=}^{78}Se)$ (the E–D splitting in ref. 3) at different electron correlation treatment levels used for the shielding surface. (a) The nonrelativistic (NR) level. (b) Relativistic corrections at the 4-component (D-B3LYP) as well as 1- and 2-electron [B3LYP(1 + 2)] BPPT levels of theory; with different DFT functionals. (c) The total results containing NR data with CCSD and CCSD(T) and the relativistic BPPT(1) contributions at the B3LYP level. The NR CCSD(T) result is also shown with D-B3LYP and BPPT corrections including both 1- and 2-electron spin–orbit contributions [B3LYP(1 + 2)]. Also NR + BPPT(1) results with different DFT functionals are displayed.

include the SOO but only the SSO contributions there is room for other sources of difference between the D-B3LYP and B3LYP(BPPT) data. One such source may be the different treatment of the gauge origin problem in the two methods: the BPPT

 

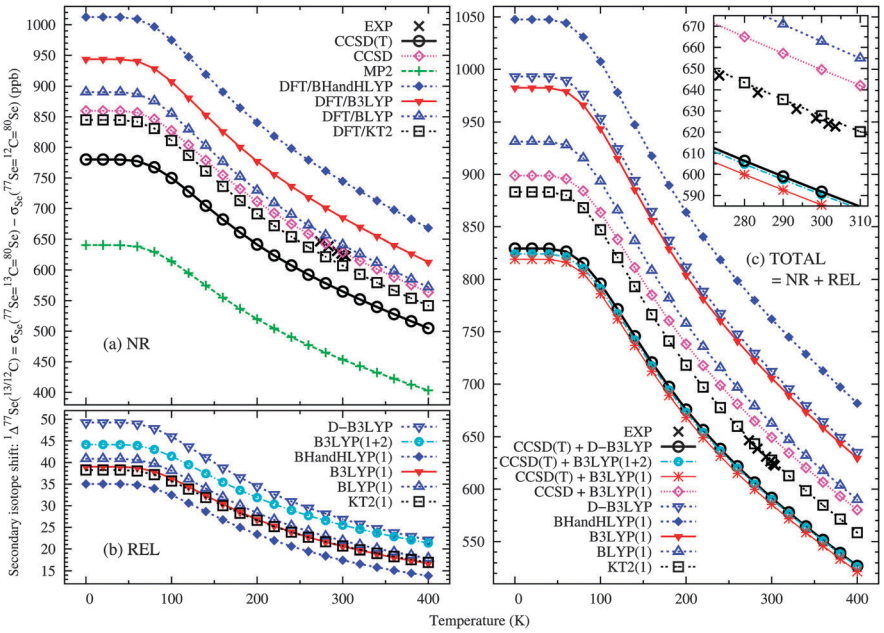


**Fig. 2** As in Fig. 1 but for the one-bond secondary $^{77}$Se isotope shift: $^1\Delta^{77}Se(^{13/12}C) = \sigma_{Se}(^{77}Se{=}^{13}C{=}^{80}Se) - \sigma_{Se}(^{77}Se{=}^{12}C{=}^{80}Se)$ (the E′–E splitting in ref. 3).

calculations are done with a common gauge origin and Dirac-DFT with GIAO. Nonetheless, the perturbational relativistic method is sufficiently accurate for treating the small relativistic corrections for the secondary $^{77}$Se isotope shifts in $CSe_2$. This is not necessarily the case in general in systems with heavy elements, which eventually will call for a fully relativistic treatment. In addition, more complex molecules with larger electron correlation effects may in some cases necessitate *ab initio* treatment of electron correlation, also for the relativistic contributions.[4,5,29,31,32]

A substantial overestimation of the secondary $^{77}$Se isotope shifts occurs due to the use of a smaller VQZ basis in the CCSD(T) calculation of the force field (see Table 3) when used together with the best current NR[CCSD(T)] and REL(D-B3LYP) shielding surfaces. This indicates that modeling of the isotope shift in $CSe_2$ is very demanding, as only the best current, CCSD(T)/V5Z force field places the NR[CCSD(T)] data in a position a bit below the experimental data. This enables the positive relativistic corrections to approach the experiment from below. The slight underestimation in our best CCSD(T) + D-B3LYP-model with respect to the experimental shifts, is most likely due to deficiencies in the basis set, the electron correlation treatment (mainly at the REL level), as well as the description of the force field. Against this background, the on-the-spot BPPT(1) results by BLYP and KT2 functionals in Fig. 1 and 2, respectively, are partly coincidental, particularly when recalling that a full 4-component treatment would increase the results.

A more detailed analysis of the BPPT-5 terms, including also the 2-electron SO-I contributions (see Fig. S1–S4 in ESI†), reveals that the reason for the peculiarly small relativistic effects in the secondary $^{77}$Se isotope shifts is due to the same reasons as the overall smallness of the relativistic effect on $^{77}$Se shielding, as discussed above. There is a heavy mutual cancellation among the SO-I terms, enhanced by the 2-electron FC-I(2) term. This leaves the small and negative SO-I rovibrational contribution to reduce the impact of the somewhat larger and positive REL-*p* term.

Apart from the magnitude, the relativistic contribution improves also the temperature dependence of the secondary isotope effect. This is demonstrated in the temperature derivatives of the secondary isotope shifts around room temperature (see Table S3 in ESI†). The temperature dependence of the secondary $^{77}$Se isotope shift due to the change of carbon isotope, the E′–E splitting, is mainly affected by the $\langle\sigma^{Se}_{\theta\theta}\rangle^T$ term in both the NR and REL parts [see panels (d) and (e) in Fig. S3 in ESI†]. However, among the REL terms the only other significant contribution is $\langle\sigma^{Se}_{r'}\rangle^T$. In the NR terms all the first- and second-order stretching contributions (other than $\langle\sigma^{Se}_{r'r'}\rangle^T$) have sizable magnitudes, although they do not cause much temperature dependence. That is in a clear contrast to the secondary $^{77}$Se shift due to the mass differences in the other Se atom [such as the E–D splitting, see panels (d) and (e) in Fig. S1 in ESI†]. The magnitude of the latter is mainly dictated by the $\langle\sigma^{Se}_{r'}\rangle^T$ term of eqn (4), *i.e.*, the "remote" C═Se bond stretch. This term plays also the main role in the temperature dependence of the two-bond isotope splitting, together with the smaller, second-order $\langle\sigma^{Se}_{rr}\rangle^T$ and $\langle\sigma^{Se}_{\theta\theta}\rangle^T$ terms. Compared with the experimental temperature derivatives of the isotope splittings ($d^1\Delta^{77}Se_{E'-E}/dT = -0.80$ ppb K$^{-1}$ and $d^2\Delta^{77}Se_{E-D}/dT = -0.040$ ppb K$^{-1}$) at room temperature,[3] our NR/REL = CCSD(T)/DB3LYP (−0.732 ppb K$^{-1}$ and −0.040 ppb K$^{-1}$) and CCSD(T)/BPPT[B3LYP(1 + 2)] (−0.723 ppb K$^{-1}$ and −0.040 ppb K$^{-1}$) results are in excellent agreement (see Table S3 in ESI†).

### 3.3 Secondary $^{13}$C isotope shifts

The secondary $^{13}$C isotope shifts due to changes in the Se isotopes[3] are listed in Table 4. Fig. 3 displays the magnitude and temperature

**Table 4** Experimental and theoretical secondary $^{13}C$ isotope shifts in $CSe_2$ at 300 K[a]

| NR[b] | Line[c] | KT2 | BLYP | B3LYP | BHandHLYP | MP2 | CCSD | CCSD(T) | CCSD(T)/VQZ[d] |
|---|---|---|---|---|---|---|---|---|---|
| $^1\Delta^{13}C(^{74}Se,^{78}Se)$ | A | −1.9 | −2.1 | −2.7 | −3.6 | 0.1 | −2.9 | −2.0 | −2.3 |
| $^1\Delta^{13}C(^{76}Se,^{76}Se)$ | A | −1.8 | −2.0 | −2.5 | −3.4 | 0.1 | −2.8 | −1.9 | −2.2 |
| $^1\Delta^{13}C(^{74}Se,^{80}Se)$ | B | −0.2 | −0.2 | −0.3 | −0.3 | 0.0 | −0.3 | −0.2 | −0.2 |
| $^1\Delta^{13}C(^{74}Se,^{82}Se)$ | C | 1.4 | 1.6 | 2.1 | 2.7 | −0.1 | 2.3 | 1.6 | 1.8 |
| $^1\Delta^{13}C(^{76}Se,^{80}Se)$ | C | 1.7 | 1.9 | 2.4 | 3.2 | −0.1 | 2.7 | 1.8 | 2.1 |
| $^1\Delta^{13}C(^{78}Se,^{78}Se)$ | C | 1.8 | 2.0 | 2.5 | 3.4 | −0.1 | 2.8 | 1.9 | 2.2 |
| $^1\Delta^{13}C(^{76}Se,^{82}Se)$ | D | 3.3 | 3.7 | 4.7 | 6.3 | −0.2 | 5.2 | 3.6 | 4.0 |
| $^1\Delta^{13}C(^{78}Se,^{80}Se)$ | D | 3.4 | 3.9 | 5.0 | 6.6 | −0.2 | 5.5 | 3.8 | 4.2 |
| $^1\Delta^{13}C(^{78}Se,^{82}Se)$ | E | 5.0 | 5.8 | 7.3 | 9.7 | −0.3 | 8.0 | 5.5 | 6.2 |
| $^1\Delta^{13}C(^{80}Se,^{80}Se)$ | E | 5.1 | 5.8 | 7.4 | 9.9 | −0.3 | 8.1 | 5.6 | 6.3 |
| $^1\Delta^{13}C(^{80}Se,^{82}Se)$ | F | 6.7 | 7.7 | 9.7 | 12.9 | −0.3 | 10.7 | 7.4 | 8.3 |
| REL[e] | | KT2 | BLYP | B3LYP | BHandHLYP | B3LYP-5[f] | B3LYP(1&2)[g] | D-B3LYP[h] | D-B3LYP/VQZ[d,h] |
| $^1\Delta^{13}C(^{74}Se,^{78}Se)$ | A | 1.2 | 1.2 | 1.4 | 1.6 | 1.4 | 1.2 | 1.1 | 1.2 |
| $^1\Delta^{13}C(^{76}Se,^{76}Se)$ | A | 1.2 | 1.2 | 1.3 | 1.6 | 0.1 | 1.2 | 1.1 | 1.2 |
| $^1\Delta^{13}C(^{74}Se,^{80}Se)$ | B | 0.1 | 0.1 | 0.1 | 0.2 | −1.1 | 0.1 | 0.1 | 0.1 |
| $^1\Delta^{13}C(^{74}Se,^{82}Se)$ | C | −1.0 | −1.0 | −1.1 | −1.3 | 1.3 | −0.9 | −0.9 | −0.9 |
| $^1\Delta^{13}C(^{76}Se,^{80}Se)$ | C | −1.1 | −1.1 | −1.2 | −1.5 | −1.2 | −1.1 | −1.0 | −1.1 |
| $^1\Delta^{13}C(^{78}Se,^{78}Se)$ | C | −1.2 | −1.2 | −1.3 | −1.6 | −2.4 | −1.2 | −1.1 | −1.2 |
| $^1\Delta^{13}C(^{76}Se,^{82}Se)$ | D | −2.2 | −2.2 | −2.4 | −2.9 | −1.3 | −2.2 | −2.0 | −2.2 |
| $^1\Delta^{13}C(^{78}Se,^{80}Se)$ | D | −2.3 | −2.3 | −2.6 | −3.0 | −2.5 | −2.3 | −2.1 | −2.3 |
| $^1\Delta^{13}C(^{78}Se,^{82}Se)$ | E | −3.4 | −3.4 | −3.7 | −4.4 | −3.7 | −3.4 | −3.0 | −3.3 |
| $^1\Delta^{13}C(^{80}Se,^{80}Se)$ | E | −3.4 | −3.4 | −3.8 | −4.5 | −3.8 | −3.4 | −3.1 | −3.4 |
| $^1\Delta^{13}C(^{80}Se,^{82}Se)$ | F | −4.5 | −4.5 | −5.0 | −5.9 | −5.0 | −4.5 | −4.0 | −4.5 |
| TOTAL[i] | | KT2 | BLYP | B3LYP | BHandHLYP | D-B3LYP | CCSD(T) + D-B3LYP | CCSD(T) + D-B3LYP/VQZ[d] | Exp.[c] |
| $^1\Delta^{13}C(^{74}Se,^{78}Se)$ | A | −0.6 | −0.9 | −1.3 | −1.9 | −1.4 | −0.9 | −1.1 | −1.2 |
| $^1\Delta^{13}C(^{76}Se,^{76}Se)$ | A | −0.6 | −0.8 | −1.2 | −1.8 | −1.4 | −0.9 | −1.0 | −1.2 |
| $^1\Delta^{13}C(^{74}Se,^{80}Se)$ | B | −0.1 | −0.1 | −0.1 | −0.2 | −0.1 | −0.1 | −0.1 | 0.0 |
| $^1\Delta^{13}C(^{74}Se,^{82}Se)$ | C | 0.5 | 0.7 | 1.0 | 1.5 | 1.1 | 0.7 | 0.8 | 1.1 |
| $^1\Delta^{13}C(^{76}Se,^{80}Se)$ | C | 0.6 | 0.8 | 1.2 | 1.8 | 1.3 | 0.8 | 1.0 | 1.1 |
| $^1\Delta^{13}C(^{78}Se,^{78}Se)$ | C | 0.6 | 0.8 | 1.2 | 1.8 | 1.4 | 0.9 | 1.0 | 1.1 |
| $^1\Delta^{13}C(^{76}Se,^{82}Se)$ | D | 1.1 | 1.5 | 2.3 | 3.4 | 2.5 | 1.6 | 1.9 | 2.2 |
| $^1\Delta^{13}C(^{78}Se,^{80}Se)$ | D | 1.1 | 1.6 | 2.4 | 3.6 | 2.7 | 1.7 | 2.0 | 2.2 |
| $^1\Delta^{13}C(^{78}Se,^{82}Se)$ | E | 1.7 | 2.4 | 3.5 | 5.3 | 3.9 | 2.5 | 2.9 | 3.3 |
| $^1\Delta^{13}C(^{80}Se,^{80}Se)$ | E | 1.7 | 2.4 | 3.6 | 5.4 | 4.0 | 2.6 | 2.9 | 3.3 |
| $^1\Delta^{13}C(^{80}Se,^{82}Se)$ | F | 2.2 | 3.2 | 4.7 | 7.0 | 5.2 | 3.4 | 3.8 | 4.4 |

[a] In ppb. Present data with the CCSD(T)/V5Z force field with $r_e$ = 1.6881 Å unless otherwise noted. Isotope shifts with respect to the $^{76}Se{=}{=}^{13}C{=}{=}^{78}Se$ isotopomer. [b] Present nonrelativistic (NR) calculations with the HIV/FIV basis set for C/Se used for the shielding surfaces. [c] Experimental spectral lines as denoted in ref. 3, measured in $C_6D_6$ solution. [d] Present calculations with the CCSD(T)/VQZ force field with $r_e$ = 1.6890 Å. [e] Present relativistic (REL) contributions with the HIVu6/FIVu6 basis set for C/Se. Computed at the 1-electron BPPT level of theory unless otherwise noted. [f] Present results including only the main relativistic 1-electron BPPT-5 terms.[45] [g] Present relativistic BPPT contribution including both 1- and 2-electron SO-I terms. [h] Present four-component D-DFT relativistic contributions with the B3LYP functional (D-B3LYP – NR-B3LYP). [i] Present total isotope shift (TOTAL = NR + REL).

dependence of the E–D splitting in ref. 3 of the $^{13}C$ NMR spectrum [$^1\Delta^{13}C(^{80/78}Se) = \sigma_C(^{80}Se{=}{=}^{13}C{=}{=}^{80}Se) - \sigma_C(^{78}Se{=}{=}^{12}C{=}{=}^{80}Se)$]. These shifts have been analyzed before,[4] including relativistic corrections from the SO-I terms. Here we complement the picture by a high-accuracy NR treatment as well as a more complete analysis of REL terms. The analysis by BPPT shows that no such cancellation of the different contributions takes place for $^{13}C$ as for $^{77}Se$. The decrease of relativistic effect on $^{13}C$ isotope shift by SR paramagnetic (REL-*p*) terms is negligible and, as already studied in ref. 4, the SO-I, mainly FC-I, spin–orbit relativistic contributions are responsible for the significant −50% reduction (as compared to NR data) of the total isotope shift, as estimated with the D-DFT(GIAO) method with the B3LYP functional. Obviously, the relativistic changes in the temperature derivatives of the secondary isotope shifts around room temperature (Table S3 in ESI†) behave similarly. The detailed analysis in ref. 4 of the roles of the different terms in the expansion in displacement coordinates in eqn (4) still holds.

### 3.4 Finite-temperature averages of the $^{77}Se$ and $^{13}C$ shielding constants

In Fig. 4, the rovibrational effects on $^{77}Se$ and $^{13}C$ shielding constants are displayed. The demands placed on the correlation treatment of the dominant NR contribution are severe for both shieldings as shown in Fig. 4(a and d): the MP2 method grossly underestimates (by *ca.* 20% and 50%, respectively) the thermal effects on $^{77}Se$ and $^{13}C$ shieldings and even CCSD overestimates them by about 10% and 30%, respectively. The best DFT functional, KT2, performs similarly to CCSD for $^{77}Se$ while for $^{13}C$ shielding KT2 is in a very good agreement with the CCSD(T) result. The DFT overestimation systematically increases with the exact HF exchange in the BLYP → B3LYP → BHandHLYP series

 

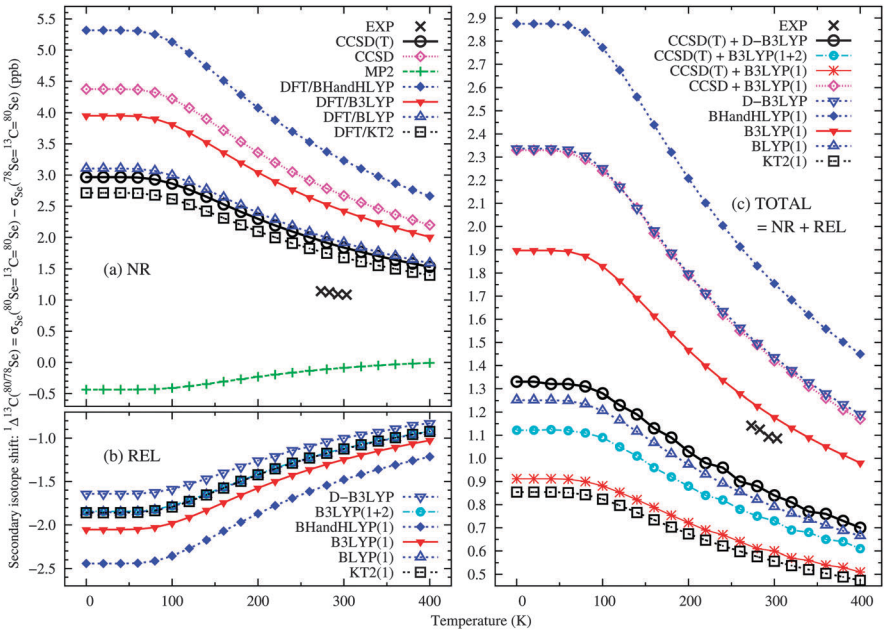


**Fig. 3** As in Fig. 1 but for the one-bond secondary $^{13}C$ isotope shift: $^1\Delta^{13}C(^{80/78}Se) = \sigma_C(^{80}Se{=}^{13}C{=}^{80}Se) - \sigma_C(^{78}Se{=}^{12}C{=}^{80}Se)$ (the E–D splitting in ref. 3).

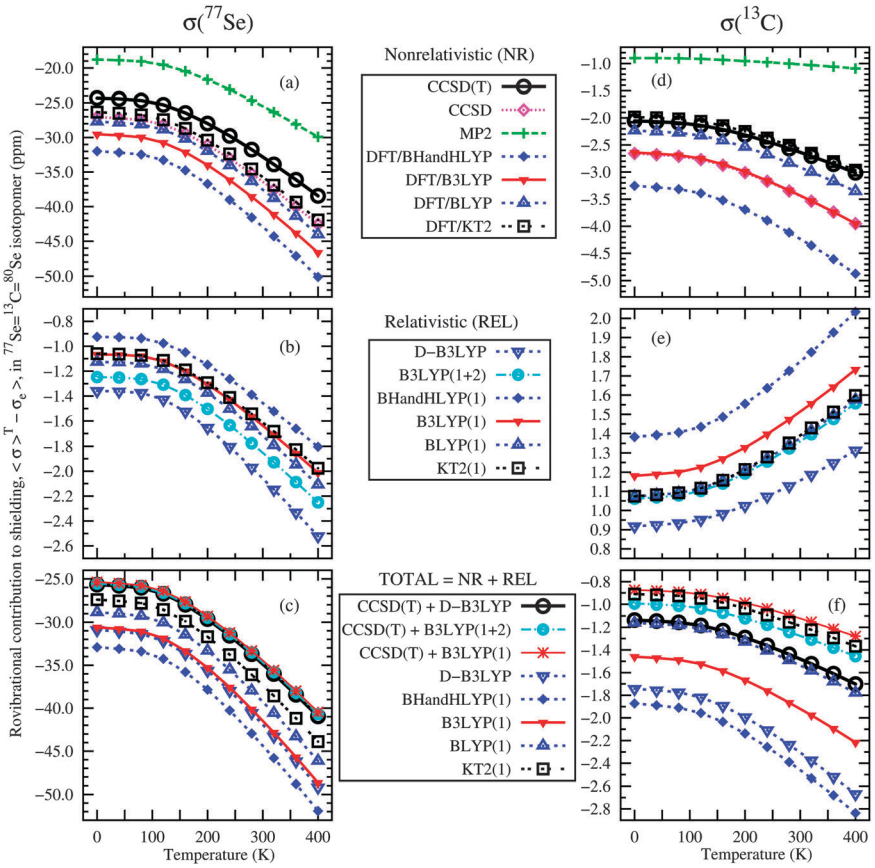


**Fig. 4** The temperature dependence of $^{77}Se$ [panels (a)–(c)] and $^{13}C$ [panels (d)–(f)] shielding constants in $^{77}Se{=}^{13}C{=}^{80}Se$ isotopomer at different electron correlation treatment levels. (a, d) The nonrelativistic (NR) level. (b, e) Relativistic corrections at the 4-component (D-B3LYP) as well as 1- and 2-electron [B3LYP(1 + 2)] BPPT levels of theory; with different DFT functionals. (c, f) The total results containing NR data with CCSD(T) and the relativistic BPPT(1) contributions at the B3LYP level. The NR CCSD(T) result is also shown with D-B3LYP and BPPT corrections including both 1- and 2-electron spin–orbit contributions [B3LYP(1 + 2)]. Also NR + BPPT(1) results with different DFT functionals are displayed.

of functionals, with the last one producing even larger errors than MP2 for both shieldings.

As clearly displayed in Fig. 4(a–c), the rovibrational effects on $^{77}$Se shielding occur mainly due to the NR contributions. Relativity is only seen to increase the rovibrational contribution to Se shielding by a couple of percent. As observed earlier in $XeF_2$,[5] although there are differences between the different DFT functionals in the predicted relativistic contribution to the rovibrational effects on the shielding of the heavy nucleus, the range of these variations is relatively narrow on the scale of the total observable. Hence, it should be safe to model relativity at the DFT level with all the current functionals. An increasing admixture of the exact HF exchange decreases the REL effect. The 4-component D-B3LYP result is slightly larger than BPPT result with the same functional. The latter usually only includes the important 1-electron, third-order spin–orbit, FC-I(1) and SD-I(1) contributions. However, as mentioned above, D-B3LYP also includes the 2-electron SSO contribution, which may partly explain the difference. Indeed, when including those and also the SOO contributions in the leading-order, 2-electron FC-I(2) and SD-(2) terms, the B3LYP(1 + 2) result in Fig. 4(b) comes much closer to the D-B3LYP result. The remaining difference is, in addition to the obvious methodology difference, probably also due to the fact that BPPT result is not obtained with GIAOs but with a common gauge origin placed at the Se nucleus in question. However, the overall results show that the BPPT approximation is adequate for treating relativistic effects on $^{77}$Se shielding (chemical shift) in $CSe_2$.

The positive relativistic (REL) correction illustrated in Fig. 4(e) almost halves the negative ZPV and thermal effects on $^{13}$C shielding ($^{77}$Se═$^{13}$C═$^{80}$Se isotopomer). The REL correction of $^{13}$C shielding constant increases with temperature, similarly to what was observed for $^{19}$F in $XeF_2$ (ref. 5) and, hence, cancels with the magnitude and temperature dependence due to the NR contribution. This is opposite to what is observed for the heavy-element shift, for $^{77}$Se in $CSe_2$ and, as reported earlier, for Xe in $XeF_2$.[5] The detailed BPPT analysis reveals that both the SR REL-*p* and SD spin–orbit (SD-I) terms only have a minor role in the overall relativistic effects. Hence, the FC-I contribution suggested in ref. 4 is confirmed here to be the dominant one in both the rovibrational contributions to $^{13}$C shielding and the secondary isotope shifts of this nucleus. The KT2 and BLYP functionals produce very similar REL corrections at BPPT(1) level of theory, while an increasing admixture of the exact HF exchange considerably increases the REL effect. Also the overestimation of REL effect by 1-electron BPPT, B3LYP(1), is relatively large when compared to D-B3LYP results. The REL effect in the case of $^{13}$C shielding is almost purely due to SO effects (see below) including the 2-electron SO-I terms, mainly FC-I(2). They render the computational results clearly nearer to the D-B3LYP results. With reference to the SOO/SSO discussion above, the truth lies somewhere between the two relativistic methods. However, the quality of electron correlation treatment is the more important aspect for the overall accuracy, which leaves room for the *ab initio* correlation treatment of also the relativistic terms.

The origins of the temperature dependence in terms of the average displacement coordinates are displayed more closely in Fig. S7 and S9 in ESI,† respectively. Fig. S8 and S10 in ESI† show the temperature dependence of the relativistic BPPT contributions to the rovibrational averages. The shielding parameters of the property hypersurfaces are tabulated in Tables S4 and S5 of ESI.† While all terms of the expansion in displacement coordinates in eqn (4) are contributing to the rovibrational average of $^{77}$Se shielding (see Fig. S7 and Table S4 in ESI†), especially at the NR level the largest contribution and most of the temperature dependence is caused by the $\langle\sigma^T_{\theta\theta}\rangle$ term. While at the NR level also the first-order stretching coordinates (*e.g.* $\langle\sigma^T_r\rangle$ and $\langle\sigma^T_{r'}\rangle$) are important, the REL contribution is almost entirely due to the $\langle\sigma^T_{\theta\theta}\rangle$ term with the only other important, yet much smaller contribution from the $\langle\sigma^T_{r'}\rangle$ term. This is because the SR paramagnetic contribution (REL-*p*) cancels the spin–orbit (SO-I) terms in all other degrees of freedom (see Fig. S8 in ESI†).

Also in the case of $^{13}$C shielding, the $\langle\sigma^T_r\rangle$ and $\langle\sigma^T_{r'}\rangle$ terms dictate the magnitude and temperature dependence at both NR and REL levels (see Fig. S9 and Table S5 in ESI†). In addition, the $\langle\sigma^T_{\theta\theta}\rangle$ term plays a significant role in temperature dependence, especially at the NR level. The origins of the REL effects and their temperature dependence follow those of the dominating FC spin–orbit (FC-I) contribution (see Fig. S10 in ESI†).

The above-discussed relativistic and correlation effects apply also to the temperature derivatives around room temperature for $^{77}$Se and $^{13}$C shieldings, shown in Table S6 in ESI.† The notable relativistic correction increases the negative temperature derivative of $^{77}$Se shielding by about 10%. Relativity is even more important for the negative $^{13}$C shielding derivative, which, in contrast, is about 40% smaller than at NR level. As already discussed in ref. 4, the $^{13}$C shielding derivative is far from the experimental result obtained in solution phase[3] completely unlike the isotope shift. This adds to the evidence obtained for instance for $^{129}$Xe and $^{19}$F shieldings in $XeF_2$,[5] that the thermal dependence of absolute shieldings is sensitive to solvent effects and, hence, not directly suited for comparison with pure rovibrational modeling *in vacuo*.

## 4 Conclusions

Temperature effects due to rovibrational motion on the NMR absolute shielding constants and secondary isotope shifts of $^{77}$Se and $^{13}$C nuclei were studied in the $CSe_2$ molecule. This was carried out with high-level *ab initio* modeling of both the property hypersurfaces and the cubic anharmonic force field of the compound, which were combined to obtain a quantum-mechanical treatment of the thermal effects. The descriptions of electron correlation as well as relativistic effects on the property hypersurfaces were studied in detail. The relativistic effects on the shielding surfaces were treated at both perturbational (BPPT) and fully relativistic (4-component Dirac) levels of theory.

We have shown that the NMR shielding surfaces in $CSe_2$ possess significant correlation effects as even the CCSD method substantially deviates from the benchmark CCSD(T) results at

 

the nonrelativistic level of theory, and the MP2 method gives clearly unrealistic shielding surfaces. Although quite a wide range of NR results is obtained with the different currently used DFT functionals, the results are systematic and present no such drastic failure as observed earlier for $XeF_2$.[5]

The modest absolute errors in the quite small relativistic corrections produced by the different DFT functionals suggest that DFT provides reasonable estimates for secondary $^{77}$Se isotope shifts. The two-electron spin–orbit effects are needed in the perturbational relativistic BPPT method for approaching the rovibrational corrections obtained by the fully relativistic D-DFT method. The perturbational analysis shows that the same five perturbational terms that have earlier been found to mostly affect chemical shifts are also responsible for the rovibrational effects on both $^{77}$Se and $^{13}$C nuclear magnetic shieldings. Not only the spin–orbit contributions but also the scalar relativistic paramagnetic contributions have a significant role in the thermal averages of shielding, especially for $^{77}$Se.

The currently used piece-wise approach that combines high-level *ab initio* NR property hypersurface with a relativistic modification by DFT leads to a quantitative accuracy for the secondary isotope shifts of the heavy $^{77}$Se nucleus. However, the comparatively large role of relativistic influences (due to the small value of the shielding constant in this case) leaves room for improvement in the parameters of the light $^{13}$C nucleus. Not quite the same level of accuracy is reached for $^{13}$C as for $^{77}$Se. The reason for good-quality secondary $^{77}$Se isotope shifts already at the NR level is shown to be the coincidental small relativistic correction. The smallness is caused by the heavy mutual cancellation of the scalar and spin–orbit relativistic effects in $CSe_2$. The best presently studied DFT functional, KT2, performs reasonably well at both the NR and REL levels of theory for both $^{77}$Se and $^{13}$C nuclei.

The remaining, small deviations from the experiment may be related to deficiencies in the potential energy surface, as well as the relativistic part of the shielding surface, especially in the case of $^{13}$C. The present method with its well-controlled approximations for electron correlation provides high-quality estimates for the demanding isotope shifts. We expect that the same is true also for thermal effects on the absolute shieldings of an unsolvated $CSe_2$ molecule, for which experimental data are lacking. As discussed before, the latter parameter is affected by significant solvent effects in solution state measurements.

## Acknowledgements

We thank the Academy of Finland (PL and JV), Tauno Tönning Fund, and U. Oulu (JV) for funding. Computations were partially carried out at CSC – IT Center for Science Ltd (Espoo, Finland), partially using the facilities of the Finnish Grid Initiative.

## References

1 C. J. Jameson, in *Theoretical Models of Chemical Bonding. Part 3. Molecular Spectroscopy, Electronic Structure, and Intramolecular Interactions*, ed. Z. B. Maksic, Springer, Berlin, 1991, p. 457.
2 J. P. Jokisaari, L. P. Ingman, G. J. Schrobilgen and J. C. P. Sanders, *Magn. Reson. Chem.*, 1994, **32**, 242.
3 J. Lounila, J. Vaara, Y. Hiltunen, A. Pulkkinen, J. Jokisaari and M. Ala-Korpela, *J. Chem. Phys.*, 1997, **107**, 1350.
4 P. Lantto, J. Vaara, A. M. Kantola, V.-V. Telkki, B. Schimmelpfennig, K. Ruud and J. Jokisaari, *J. Am. Chem. Soc.*, 2002, **124**, 2762.
5 P. Lantto, S. Kangasvieri and J. Vaara, *J. Chem. Phys.*, 2012, **137**, 214309.
6 T. Helgaker, M. Jaszuński and K. Ruud, *Chem. Rev.*, 1999, **99**, 293.
7 T. A. Ruden and K. Ruud, in *Calculation of NMR and EPR Parameters: Theory and Applications*, ed. M. Kaupp, M. Bühl and V. G. Malkin, Wiley-VCH, Weinheim, 2004, pp. 153–174.
8 T. Helgaker, S. Coriani, P. Jørgensen, K. Kristensen, J. Olsen and K. Ruud, *Chem. Rev.*, 2012, **112**, 543.
9 S. Grigoleit and M. Bühl, *Chem.–Eur. J.*, 2004, **10**, 5541.
10 M. Bühl, P. Imhof and M. Repisky, *ChemPhysChem.*, 2004, **5**, 410.
11 M. Bühl and F. T. Mauschick, *Magn. Reson. Chem.*, 2004, **42**, 737.
12 S. Grigoleit and M. Bühl, *J. Chem. Theor. Comput.*, 2005, **1**, 181.
13 J. C. Davis, M. Bühl and K. R. Koch, *J. Chem. Theor. Comput.*, 2012, **8**, 1344.
14 K. Ruud, J. Vaara, J. Lounila and T. Helgaker, *Chem. Phys. Lett.*, 1998, **297**, 467.
15 J. Vaara, J. Lounila, K. Ruud and T. Helgaker, *J. Chem. Phys.*, 1998, **109**, 8388.
16 A. M. Kantola, S. Ahola, J. Vaara, J. Saunavaara and J. Jokisaari, *Phys. Chem. Chem. Phys.*, 2007, **9**, 481.
17 A. M. Kantola, P. Lantto, J. Vaara and J. Jokisaari, *Phys. Chem. Chem. Phys.*, 2010, **12**, 2679.
18 H. Nakatsuji, H. Takashima and M. Hada, *Chem. Phys. Lett.*, 1995, **233**, 95.
19 J. Vaara, K. Ruud, O. Vahtras, H. Ågren and J. Jokisaari, *J. Chem. Phys.*, 1998, **109**, 121.
20 M. Kaupp, O. L. Malkina, V. G. Malkin and P. Pyykkö, *Chem.–Eur. J.*, 1998, **4**, 118.
21 J. Vaara, K. Ruud and O. Vahtras, *J. Chem. Phys.*, 1999, **111**, 2900.
22 B. Minaev, J. Vaara, K. Ruud, O. Vahtras and H. Ågren, *Chem. Phys. Lett.*, 1998, **295**, 455.
23 B. Cromp, T. Carrington, D. R. Salahub, O. L. Malkina and V. G. Malkin, *J. Chem. Phys.*, 1999, **110**, 7153.
24 P. Lantto and J. Vaara, *J. Chem. Phys.*, 2001, **114**, 5482.
25 P. Lantto, J. Vaara and T. Helgaker, *J. Chem. Phys.*, 2002, **117**, 5998.
26 J. Vaara, *Phys. Chem. Chem. Phys.*, 2007, **9**, 5399.
27 T. W. Keal and D. J. Tozer, *J. Chem. Phys.*, 2003, **119**, 3015.
28 T. W. Keal, D. J. Tozer and T. Helgaker, *Chem. Phys. Lett.*, 2004, **391**, 374.
29 P. Lantto and J. Vaara, *J. Chem. Phys.*, 2007, **127**, 084312.
30 M. Straka, P. Lantto, M. Räsänen and J. Vaara, *J. Chem. Phys.*, 2007, **127**, 234314.
31 P. Lantto, S. Standara, S. Riedel, J. Vaara and M. Straka, *Phys. Chem. Chem. Phys.*, 2012, **14**, 10944.

32 J. Roukala, A. F. Maldonado, J. Vaara, G. A. Aucar and P. Lantto, *Phys. Chem. Chem. Phys.*, 2011, **13**, 21016.
33 J. Vaara, P. Manninen and P. Lantto, in *Calculation of NMR and EPR Parameters: Theory and Applications*, ed. M. Kaupp, M. Bühl and V. G. Malkin, Wiley-VCH, Weinheim, 2004, pp. 209–226.
34 P. Manninen, P. Lantto, K. Ruud and J. Vaara, *J. Chem. Phys.*, 2003, **119**, 2623.
35 P. Manninen, K. Ruud, P. Lantto and J. Vaara, *J. Chem. Phys.*, 2005, **122**, 114107; P. Manninen, K. Ruud, P. Lantto and J. Vaara, *J. Chem. Phys.*, 2006, **124**, 149901 (Erratum).
36 J. I. Melo, M. C. Ruiz de Azúa, C. G. Giribet, G. A. Aucar and R. H. Romero, *J. Chem. Phys.*, 2003, **118**, 471.
37 J. I. Melo, M. C. Ruiz de Azúa, C. G. Giribet, G. A. Aucar and P. F. Provasi, *J. Chem. Phys.*, 2004, **121**, 6798.
38 P. Lantto, R. H. Romero, S. S. Gómez, G. A. Aucar and J. Vaara, *J. Chem. Phys.*, 2006, **125**, 184113.
39 M. Hanni, P. Lantto, M. Iliaš, H. J. Aa. Jensen and J. Vaara, *J. Chem. Phys.*, 2007, **127**, 164313.
40 M. Straka, P. Lantto and J. Vaara, *J. Phys. Chem. A*, 2008, **112**, 2658.
41 S. Standara, K. Maliňáková, R. Marek, J. Marek, M. Hocek, J. Vaara and M. Straka, *Phys. Chem. Chem. Phys.*, 2010, **12**, 5126.
42 M. Hanni, P. Lantto and J. Vaara, *Phys. Chem. Chem. Phys.*, 2011, **13**, 13704.
43 S. Standara, P. Kulhánek, R. Marek, J. Horníček, P. Bouř and M. Straka, *Theor. Chem. Acc.*, 2011, **129**, 677.
44 D. Gaszowski and M. Ilczyszyn, *Chem. Phys. Lett.*, 2012, **538**, 29.
45 BPPT-5 (BPPT-6 for $\Delta\sigma$) is a collective name for the five (six) numerically most important terms terms for chemical shifts and anisotropic parameters (see ref. 29 and 30): scalar relativistic paramagnetic REL-$p$ = $p$-KE/OZ + $p$/mv + $p$/Dar and spin–orbit SO-I = FC-I + SD-I (+SOS from ref. 46 for $\Delta\sigma$) contributions.
46 M. C. Ruiz de Azúa, C. G. Giribet and J. I. Melo, *J. Chem. Phys.*, 2011, **134**, 034123.
47 K. Peterson, D. Figgen, E. Goll, H. Stoll and M. Dolg, *J. Chem. Phys.*, 2003, **119**, 11113.
48 Th. H. Dunning, Jr., *J. Chem. Phys.*, 1989, **90**, 1007.
49 J. F. Stanton, J. Gauss, M. E. Harding and P. G. Szalay, *Cfour, a quantum chemical program package*, 2009.
50 H. J. Aa. Jensen, R. Bast, T. Saue, L. Visscher, V. Bakken, K. G. Dyall, S. Dubillard, U. Ekström, E. Eliav, T. Enevoldsen, T. Fleig, O. Fossgaard, A. S. P. Gomes, T. Helgaker, J. K. Lærdahl, Y. S. Lee, J. Henriksson, M. Iliaš, Ch. R. Jacob, S. Knecht, S. Komorovský, O. Kullie, C. V. Larsen, H. S. Nataraj, P. Norman, G. Olejniczak, J. Olsen, Y. C. Park, J. K. Pedersen, M. Pernpointner, K. Ruud, P. Sałek, B. Schimmelpfennig, J. Sikkema, A. J. Thorvaldsen, J. Thyssen, J. van Stralen, S. Villaume, O. Visser, T. Winther and S. Yamamoto, *DIRAC, a relativistic ab initio* electronic structure program, Release DIRAC12, 2012, see http://www.diracprogram.org.
51 M. Olejniczak, R. Bast, T. Saue and M. Pecul, *J. Chem. Phys.*, 2012, **136**, 014108.
52 P. J. Stephens, C. F. Devlin, F. J. Chabalowski and M. J. Frisch, *J. Phys. Chem.*, 1994, **98**, 11623.
53 C. Lee, W. Yang and R. G. Parr, *Phys. Rev. B: Condens. Matter Mater. Phys.*, 1988, **37**, 785.
54 DALTON, a molecular electronic structure program, Release Dalton2011, 2011, see http://daltonprogram.org/.
55 A. D. Becke, *Phys. Rev. A*, 1988, **38**, 3098.
56 A. D. Becke, *J. Chem. Phys.*, 1993, **98**, 1378.
57 S. Huzinaga, *Approximate atomic functions*, University of Alberta, Edmonton, 1971.
58 W. Kutzelnigg and U. Fleischer, M. Schindler, in *NMR Basic Principles and Progress*, ed. P. Diehl, E. Fluck, H. Günther, R. Kosfeld and J. Seelig, Springer-Verlag, Berlin, vol. 23, 1990.
59 K. Fægri, Jr. and J. Almlöf, *J. Comput. Chem*, 1986, **7**, 396.
60 H. Bürger and H. J. Willner, *J. Mol. Spectrosc.*, 1988, **128**, 221.
61 C. J. Jameson and A. K. Jameson, *Chem. Phys. Lett.*, 1987, **135**, 254.
62 Q. Chen, D. L. Freeman, J. D. Odom, P. D. Ellis, poster presented at the 36 ENC-Experimental Nuclear Magnetic Resonance Conference Boston, Massachusetts, 1995, unpublished.
63 W.-H. Pan and J. P. Fackler, *J. Am. Chem. Soc.*, 1978, **100**, 5783.
64 J. Jokisaari, P. Lazzeretti and P. Pyykkö, *Chem. Phys.*, 1988, **123**, 339.
65 G. M. Bernard, K. Eichele, G. Wu, C. W. Kirby and R. E. Wasylishen, *Can. J. Chem.*, 2000, **78**, 614.

 